

Voidage of bulk solution in a tall vertical gas evolving cell

E. L. J. COENEN, L. J. J. JANSSEN

Eindhoven University of Technology, Department of Chemical Engineering and Chemistry, Laboratory of Instrumental Analysis, Electrochemistry Group, PO Box 513, 5600 MB, Eindhoven, The Netherlands

Received 16 September 1996; revised 29 January 1997

Vertical electrolyzers with parallel-plate electrodes and with a narrow interelectrode gap or with narrow gaps between the membrane and each of the electrodes are used industrially to produce gases. Conductivity measurements were carried out with a small conductivity cell built within one compartment of the cell and just above the top of the working electrode. KOH solutions were used as electrolytes and gas bubbles were evolved at a 20-segment electrode. The effect of various parameters, including current passed through the 20-segments electrode, flow rate of liquid, temperature and nature of gas evolved, was studied. From the normalized conductivity measured, the gas voidage ε was obtained. It was found that for a bubbly flow the gas voidage just above the gas-evolving electrode is given by the relation:

$$\varepsilon/(\varepsilon_{\max} - \varepsilon) = 1.4 Q_g/Q_l$$

where ε_{\max} is the maximum voidage for gas bubbles in a solution; $\varepsilon_{\max} = 0.69$ for oxygen as well as hydrogen in a concentrated and a dilute KOH solution at different liquid flow rates. Q_g is the volumetric flow rate of gas saturated with water vapour and Q_l is the volumetric flow rate of liquid. This relation can be used to calculate the voidage distribution in the bulk solution of the cell compartment with a gas-evolving electrode.

Keywords: *Voidage, electrolyser, conductivity cell, 20-segment electrode*

List of symbols

a_1	slope of $\log \varepsilon/(\varepsilon_{\max} - \varepsilon)/\log Q_g$ curve	Q_g^*	volumetric rate of gas containing no water vapour ($\text{cm}^3 \text{s}^{-1}$)
a_2	slope of $\log a_1/Q_l$ curve	Q_l	volumetric rate of liquid ($\text{cm}^3 \text{s}^{-1}$)
F	Faraday constant (C mol^{-1})	R	ohmic resistance of solution between both electrodes of the conductivity cell (Ω)
$I_{g,p}$	current in the gas-producing cell (A)	R_p	ohmic resistance of the bubble-free solution between both electrodes of the conductivity cell (Ω)
$I_{g,s}$	current passed through a segment pair of electrodes (A)	r	normalized ohmic resistance being R/R_p
i	current density (kA m^{-2})	T	temperature (K)
n	number of electrons per molecule oxidized or reduced	T_m	temperature of solution in the conductivity cell (K)
n_s	the number of gas-evolving segment pair of electrodes	<i>Greek symbols</i>	
p_g	pressure of gas saturated with water vapour (kPa)	ε	voidage
p_d	saturation pressure of water vapour for a KOH solution (kPa)	ε_{\max}	maximum voidage
p	pressure of gas (kPa)	ε_{∞}	ε in bulk of solution
Q_g	volumetric rate of gas saturated with water vapour ($\text{cm}^3 \text{s}^{-1}$)	κ	conductivity of solution measured with the conductivity cell ($\Omega^{-1} \text{cm}^{-1}$)
		κ_p	κ for bubble-free solution ($\Omega^{-1} \text{cm}^{-1}$)

1. Introduction

Vertical electrolyzers with parallel-plate electrodes and a narrow interelectrode gap are used industrially to produce gases. A short review on ohmic resistance of solution in a vertical gas-evolving cell was recently published [1]. Experimental results on the ohmic re-

sistance of solution between a gas-evolving electrode and a nongas-evolving electrode were also given. A bubble free or a bubble containing solution was passed through the gap between these electrodes. The bubbles were evolved in a tall vertical divided gas-producing cell. However, the maximum voidage of this solution was relatively small, ~ 0.35 , because of

the 45° slope of the connecting tube between the vertical gas-producing cell and the vertical tube with the measuring cell [1]. To describe the ohmic resistance of solution within a gas-evolving cell, knowledge of the voidage of the bulk solution is necessary.

No reliable experimental results on the voidage of bulk solution in gas-evolving cells are well known. In stationary liquid the gas voidage as a function of volumetric gas flow rate for electro-generated gases is given in [2]. A maximum gas voidage has also been found [2]. In a flowing liquid the voidage of NaOH solutions containing a mixture of oxygen and hydrogen bubbles generated in an undivided cell were presented [3]. It was found that the voidage increased with increasing volumetric gas flow rate, a limiting value being reached. In alkaline solution the behaviour of the bubbles is different; hydrogen bubbles do not coalesce as easily as oxygen bubbles [4].

To determine the voidage for a single gas, experiments were carried out using a conductivity cell placed within the working electrode compartment of a gas-evolving cell. The purpose of this research is to determine the voidage in the bulk solution as a function of various parameters, such as volumetric gas and liquid flow rate, temperature and position of gas-evolving electrodes.

2. Experimental details

The experimental setup described in [5] was enlarged to two solution-circuits and the undivided cell was replaced by a divided two-compartment Perspex cell. The cell was divided by a cation-exchange membrane (Nafion[®], type 117). The working electrode as well as the counter electrode had 20 segments; each segment pair could be connected separately. The distance between the segmented working electrode and the membrane was 5.0 mm. The solution in each compartment was pumped from a solution-reservoir overflow vessel upwards. The overflow vessel was thermostatted. During a series of experiments with increasing or decreasing current the temperature of the electrolyte could not be kept constant due to changes in the heat production rate. To accurately determine the temperature of liquid passing through the conductivity cell, a temperature probe was placed in the working electrode compartment just above the conductivity cell. The voltage over the thermocouple was measured by a voltmeter (Data Precision, 2380).

A conductivity cell with two platinized-platinum plate electrodes was built in the working-electrode compartment just above the top segment of the 20-segment electrode described in [1]. The distance between the top edge of the top segment and the bottom edge of the measuring electrodes of the conductivity cell was 12 mm. The measuring electrodes were 4 mm in width and 9 mm in height, the distance between the electrodes being 10 mm. The measuring electrodes ($4 \times 9 \text{ mm}^2$) were mounted on the inner walls of a 4 mm thick Perspex frame with a hole of 10 mm in width and of 800 mm in length. This frame was sealed

with two silicon rubber sheets of 0.5 mm thickness. The cross-sectional area of the flow channel between the working electrode and membrane was 50 mm^2 .

The adjustment of the current used for gas production is described in [1]. The current for each segment pair was adjusted separately, the maximum current load for a segment pair being 2.5 A. The conductivity cell was connected to a conductivity meter (Radiometer type CDM 2d). The measured conductivity was registered by a recorder (Kipp & Zonen, type BD40).

3. Results

3.1. Introduction

The conductivity of a solution within a conductivity cell was determined for a dilute (10 wt %) and a concentrated (26 wt %) KOH solution with or without bubbles. The bubbles were produced at a segmented electrode with a total current $I_{g,p}$. Moreover, the effect of the flow rate of liquid Q_l , the temperature T , the position of the gas-evolving electrode segments, where each active segment was charged with the same current, $I_{g,s}$, and the number of gas-evolving electrode segments, n_s , used to produce a fixed volumetric gas rate, where the current of a segment $I_{g,s} = I_{g,p}/n_s$ were studied. The measured data for the conductivity of solution show a spread caused by fluctuations in the voidage. To eliminate this effect, the conductivity of solution was recorded and the average value was determined.

During electrolysis heat is produced in the electrolysis cell due to current loading. The temperature increase depends on several parameters, for instance, current, flow rate of liquid and conductivity of solution. It was found that the temperature increase can be significant and that the maximum increase of temperature was about 10 K. The increase in temperature of solution during its passage through the cell enlarges the specific conductivity of the liquid and the production rate of water vapour. Oxygen and hydrogen bubbles formed at the gas-evolving electrodes take up water vapour. This results in an additional volumetric flow rate of gas consisting of oxygen or hydrogen and water vapour. Because of the large effect of temperature increase upon the conductivity of solution, the temperature of solution was determined carefully. The position of the temperature probe was sufficiently near to the conductivity cell in the gas-producing cell to indicate the temperature of the solution in the conductivity cell.

3.2. Current and volumetric flow rate of gas containing water vapour

Figure 1 shows typical experimental results. In this Figure the ohmic resistance $R (= \kappa^{-1})$ and the temperature, T_m , of the solution within the conductivity cell are given as a function of the current $I_{g,p}$ used for the production of hydrogen. Similar results were

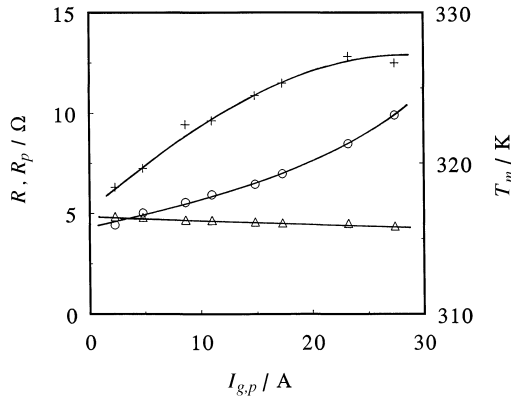


Fig. 1. Ohmic resistance R between the electrodes of the conductivity cell (+), temperature T_m just above the conductivity cell (O) and ohmic resistance of pure liquid between the electrodes of the conductivity cell at T_m (Δ) plotted against the total current $I_{g,p}$ used to produce hydrogen gas. The liquid is a 10 wt % KOH solution and its flow rate is $1.77 \text{ cm}^3 \text{ s}^{-1}$.

obtained for oxygen. It may be deduced that both R and T_m increase strongly with increasing $I_{g,p}$.

The voidage of solution was calculated using the well-known Bruggemann relation,

$$R = R_p(1 - \varepsilon)^{-3/2} \quad (1)$$

The normalized ohmic resistance, r , is defined by $r = R/R_p$, where R_p is the ohmic resistance for the bubble-free liquid. Since the ohmic resistance of solution is the inverse of the conductivity of solution, it can be shown that $r = \kappa_p/\kappa$.

The ohmic resistance, R_p , is equal to R at $I_{g,p} = 0$. To calculate ε , R_p has to be obtained at the temperature at which also R was determined. Therefore, an experimental relation between R_p and T_m was used. A typical result for R_p is also shown in Fig. 1. Evidently, R_p decreases with increasing $I_{g,p}$ due to the rise in temperature T_m .

From Fig. 1 the voidage ε , being $1 - (R_p/R)^{2/3}$, was calculated and plotted against $I_{g,p}$ in Fig. 2.

The calculated ε is the voidage of hydrogen gas containing water vapour. The water vapour content of bubbles increases with increasing $I_{g,p}$ due to the rise in liquid temperature T_m . This means that the volumetric flow rate, Q_g , of hydrogen gas containing water vapour increases more strongly than the volumetric flow rate of hydrogen gas containing no water vapour, Q_g^* . Assuming gas bubbles are saturated with water vapour, it has been shown in [1] that

$$Q_g = Q_g^* \frac{p_g - p_d}{p_g}$$

where p_d is the partial water vapour pressure and p_g is the sum of the partial pressures of gas and water vapour ($p_g = 101 \text{ kPa}$). The hydrostatic head was not taken into account in the gas volumetric calculation because its value was negligible. Q_g^* is calculated at temperature T_m .

It can be shown that at temperature T_m ,

$$Q_g^* = \frac{T_m}{298} V_{M,298} \frac{I_{g,p}}{nF}$$

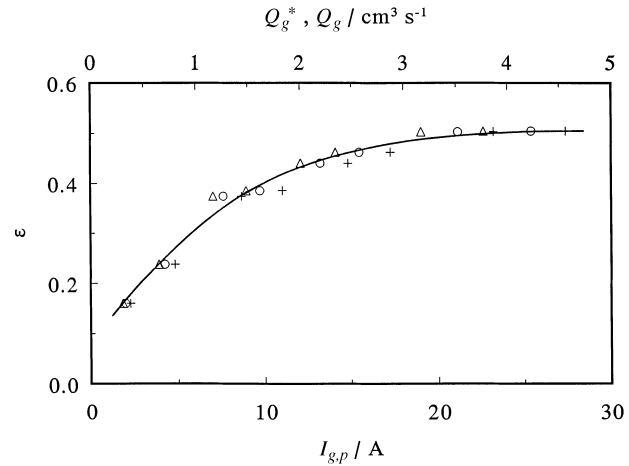


Fig. 2. Plot of gas voidage ε against the total current $I_{g,p}$ used to produce hydrogen gas (+), the volumetric rate of hydrogen gas without water vapour Q_g^* (Δ) and against the rate of hydrogen gas saturated with water vapour Q_g (O) for a 10 wt % KOH solution at the temperatures where ε has been obtained. Flow rate of liquid $1.77 \text{ cm}^3 \text{ s}^{-1}$.

Moreover, $V_{M,298} = 24.5 \times 10^3 \text{ cm}^3 \text{ mol}^{-1}$ at 298 K, $F = 96487 \text{ C mol}^{-1}$ and $n = 2$ for hydrogen and 4 for oxygen formation. Using these parameters, Q_g^* was calculated at various $I_{g,p}$.

Figure 2 shows also a typical result for the voidage, ε , as a function of Q_g for gas evolution in a KOH solution, where each segment of the 20-segments electrode was loaded with the same current, $I_{g,s}$ being $0.05 I_{g,p}$. This Figure shows that ε increases at a decreasing rate with increasing Q_g . The relation between ε and Q_g^* is also given in Fig. 2 to show the effect of water vapour formation. Comparing the ε/Q_g^* and the ε/Q_g curve both from Fig. 2, it can be concluded that the effect of water vapour is significant especially at high currents where a considerable temperature increase occurs. Since the contribution of water vapour to the voidage ε cannot be neglected, Q_g is used to obtain relations describing the effect of voidage on the solution ohmic resistance.

From Fig. 2 it also follows that ε approaches a limiting value ε_{\max} . This can be obtained by plotting the reciprocal of the voidage against the reciprocal of Q_g . Typical results are shown in Fig. 3. It follows that ε^{-1} increases linearly with Q_g^{-1} . It is likely that linear extrapolation of the $\varepsilon^{-1}/Q_g^{-1}$ curve gives ε_{\max}^{-1} . The curves of Fig. 3 intersect the ε^{-1} axis at practically the same value as ε_{\max}^{-1} . Measurements were also carried out at various solution flow rates. No systematic effect of flow rate was observed. From all the results in Fig. 3 and those for the experiments with varying solution flow rate it was found that, for both KOH solutions containing oxygen or hydrogen bubbles, the average experimental $\varepsilon_{\max} = 0.69 \pm 0.02$ based on 12 measuring points.

To obtain a relation between ε and Q_g , the factor $\varepsilon/(\varepsilon_{\max} - \varepsilon)$ is plotted against Q_g on a double logarithmic scale in Figs 4 and 5 for hydrogen and oxygen, respectively, where $\varepsilon_{\max} = 0.69$. From Figs 4 and 5 it follows that all $\log(\varepsilon/(\varepsilon_{\max} - \varepsilon)) / \log Q_g$ curves coincide and their slope, a_1 is 1.00.

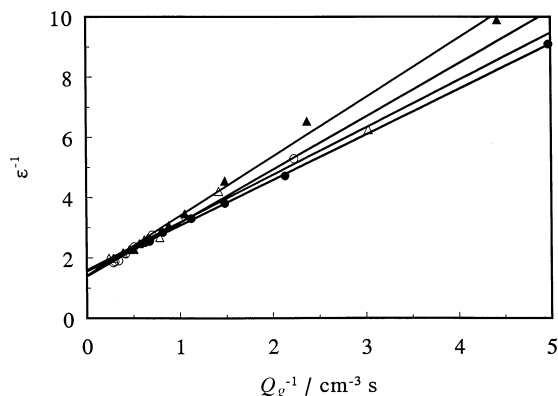


Fig. 3. Plot of ε^{-1} against the reverse of the volumetric flow rate of evolved gas saturated with water vapour (Q_g^{-1}) for hydrogen (Δ , \circ) and oxygen (\blacktriangle , \bullet) in 10 (Δ , \blacktriangle) and 26 wt % (\circ , \bullet) KOH solutions at a flow rate of liquid of $1.77 \text{ cm}^3 \text{ s}^{-1}$.

3.3. Temperature

The effect of temperature on gas voidage, ε , at $I_{g,p}$ of about 7.5 and 22 A was determined for hydrogen as well as oxygen evolution in both KOH solutions. During the series of experiments the current $I_{g,p}$ varied slightly. Since the water vapour content of the gas bubbles increases with increasing temperature, the volumetric rate of gas saturated with water vapour Q_g increases with increasing temperature at a constant current $I_{g,p}$.

To eliminate the effect of the increase in Q_g due to the temperature increase, the voidage ε at fixed rates of Q_g corresponding to 7.8 or 22.2 A at $T_m = 316 \text{ K}$ was calculated.

Results for hydrogen and oxygen evolution are shown in Figs 6 and 7, respectively. From these figures it follows that ε at constant Q_g is practically independent of temperature. The effect of the difference between the fixed rate of Q_g and the one at the conductivity measurement on ε was taken into account using the observed linearity between $\varepsilon/(\varepsilon_{\max} - \varepsilon)$ and Q_g .

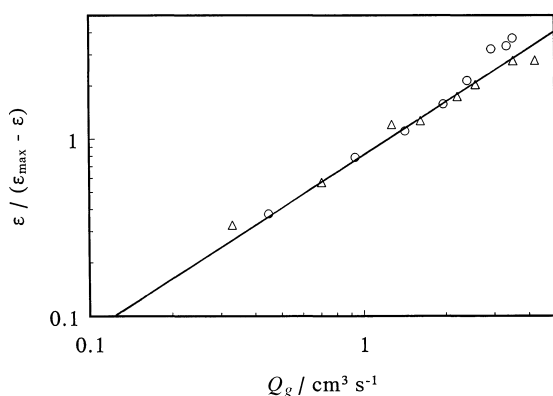


Fig. 4. Plot of $\varepsilon/(\varepsilon_{\max} - \varepsilon)$ against the volumetric flow rate of evolved gas saturated with water vapour, Q_g , on a double logarithmic scale and where $\varepsilon_{\max} = 0.69$ for hydrogen in 10 (Δ) and 26 wt % (\circ) KOH solutions at a flow rate of liquid of $1.77 \text{ cm}^3 \text{ s}^{-1}$.

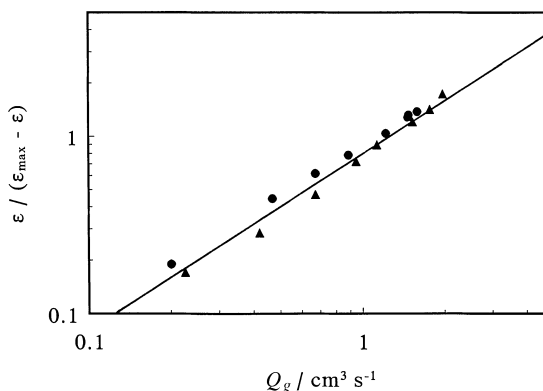


Fig. 5. Plot of $\varepsilon/(\varepsilon_{\max} - \varepsilon)$ against the volumetric flow rate of evolved gas saturated with water vapour, Q_g , on a double logarithmic scale and where $\varepsilon_{\max} = 0.69$ for oxygen in 10 (\blacktriangle) and 26 wt % (\bullet) KOH solutions at a flow rate of liquid of $1.77 \text{ cm}^3 \text{ s}^{-1}$.

3.4. Flow rate of solution

The effect of solution flow rate, Q_l on ε was determined at $I_{g,p} = 7.5$ and 22 A for hydrogen and oxygen evolution in a dilute and a concentrated KOH solution. The temperature T_m was not constant but increased sharply with decreasing Q_l . To eliminate this effect, ε at fixed values of Q_g was calculated as described in 3.3.

Results are shown in Figs 8 and 9 for hydrogen and oxygen, respectively. From these figures it follows that ε decreases with increasing flow rate, when the measuring points at the highest rate of gas evolution and the lowest rate of flow rate of solution are disregarded.

3.5. Position and number of gas-evolving segments used to produce a constant flow rate of gas

Experiments for oxygen and hydrogen in both KOH solutions at $T_m = 313 \text{ K}$ and $Q_l = 13.3 \text{ cm}^3 \text{ s}^{-1}$ were carried out, where the total current $I_{g,p}$ was fixed (i.e.,

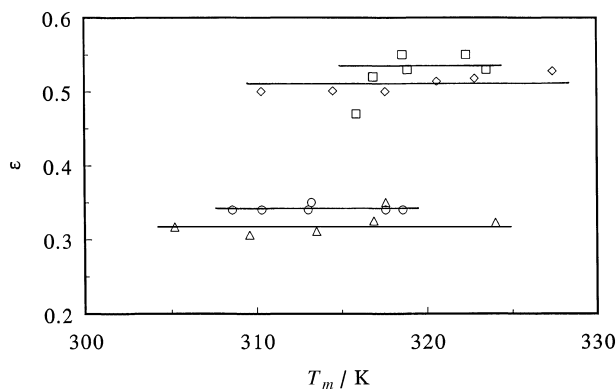


Fig. 6. Plot of ε against temperature T_m for hydrogen in a 10 and a 26 wt % KOH solution at a flow rate of liquid of $1.77 \text{ cm}^3 \text{ s}^{-1}$ and at various volumetric flow rates of hydrogen gas saturated with water vapour, namely $1.14 \text{ cm}^3 \text{ s}^{-1}$ (Δ) and $1.11 \text{ cm}^3 \text{ s}^{-1}$ (\circ) for 10 and 26 wt % KOH solution, respectively, and both values of Q_g corresponding to $I_{g,p} = 7.8 \text{ A}$ at 316 K, and 3.25 and $3.16 \text{ cm}^3 \text{ s}^{-1}$ for 10 (\diamond) and 26 wt % (\square) KOH solution, respectively, and both values of Q_g corresponding to 22.2 A at 316 K.

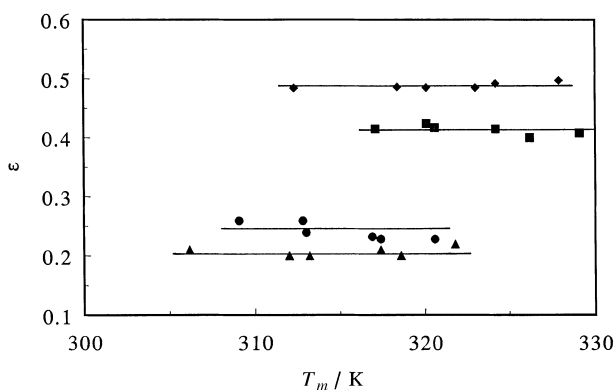


Fig. 7. Plot of ε against temperature T_m for oxygen in a 10 and a 26 wt % KOH solution at a flow rate of liquid of $1.77 \text{ cm}^3 \text{ s}^{-1}$ and at various volumetric flow rates of oxygen gas saturated with water vapour, namely, 0.57 (▲) and $0.56 \text{ cm}^3 \text{ s}^{-1}$ (●) for 10 and 26 wt % KOH solution, respectively, and both values of Q_g corresponding to 7.8 A at 316 K , and 1.63 (◆) and $1.58 \text{ cm}^3 \text{ s}^{-1}$ (■) for 10 and 26 wt % KOH solution, respectively, and both values of Q_g corresponding to 22.2 A at 316 K .

7.5 A). This current was equally distributed over different numbers of electrode segments, that is, 5, 10, 15 and 20. Moreover, the segments producing gas were localized at various heights in the cell. For instance, in the case of five gas-evolving segments, the gas-evolving segments were segments 1–5, 6–10, 11–15 and 16–20, where the segments were numbered from bottom to top in the cell. It was found that the temperature T_m and the voidage for both oxygen and hydrogen did not depend on position and on the number of gas-evolving segments at a constant total current $I_{g,p}$ for the cell.

Preliminary experiments were carried out to detect changes in gas voidage of a bubbly flow (KOH solution containing hydrogen or oxygen bubbles up to a voidage of about 0.1) during its passage through a vertical glass tube, 10 mm in diameter and 120 cm in length. The conductivity of the bubbly flow at five different heights in the tube was measured with platinized platinum-electrode pairs. The bubbly flow was formed in a tall vertical gas-producing cell and

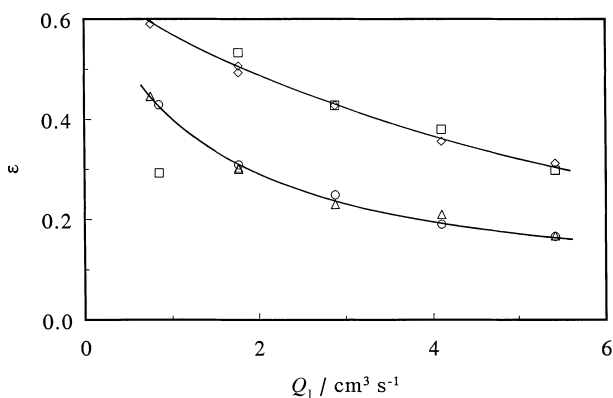


Fig. 8. Plot of ε against Q_1 for a 10 and 26 wt % KOH solution containing hydrogen bubbles at various volumetric flow rates of hydrogen gas saturated with water vapour, namely, 1.10 and $1.07 \text{ cm}^3 \text{ s}^{-1}$ for a 10 (Δ) and 26 wt % (○) KOH solution, respectively, and corresponding to $I_{g,p} = 7.5 \text{ A}$ at 318 K , and 3.37 and $3.28 \text{ cm}^3 \text{ s}^{-1}$ for a 10 (◇) and 26 wt % (□) KOH solution, respectively, and corresponding to 23 A at 318 K .

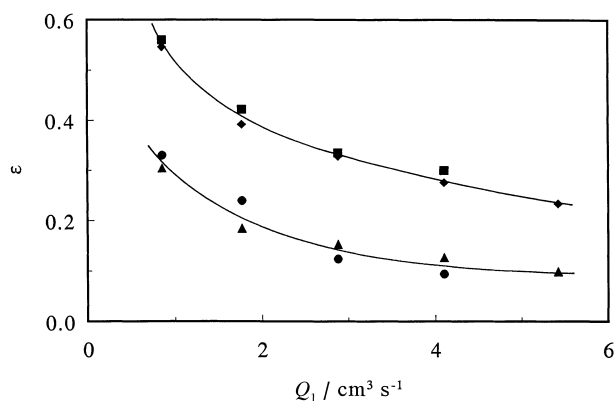


Fig. 9. Plot of ε against Q_1 for a 10 and a 26 wt % KOH solution containing oxygen bubbles at various volumetric flow rates of oxygen gas saturated with water vapour, namely, 0.55 and $0.54 \text{ cm}^3 \text{ s}^{-1}$ for a 10 (▲) and 26 wt % (●) KOH solution, respectively, and corresponding to 7.5 A at 318 K , and 1.69 and $1.64 \text{ cm}^3 \text{ s}^{-1}$ for a 10 (◆) and a 26 wt % (■) KOH solution, respectively, and corresponding to 23 A at 318 K .

was conducted through a tube with an inclination angle of 45° . In this inclined tube coalescence of bubbles occurred at the upper side of the tube particularly at low solution volumetric flow rate. No change in the conductivity of the bubbly flow was found during its passage through the long vertical tube. Thus a steady-state condition of the bubbly flow had already been established at the lowest measuring point.

4. Discussion

To achieve high gas voidages in the bulk solution, high currents and low volumetric flow rates of liquid have to be applied. As expected, the solution increased in temperature during its passage through the electrolysis cell. The largest increase in temperature was about 10 K . Appropriate corrections for increase in volume of evolved gas and for water evaporation were applied to determine the flow rate of gas saturated with water vapour, as outlined in Section 3.2.

It is likely that the volumetric flow rate of gas saturated with water vapour and the liquid flow rate are the most relevant parameters determining the gas voidage in the bulk solution. It was observed that, except under extreme conditions, the liquid–gas mixtures behave like bubbly flows, where the liquid phase is continuous and the vapour phase is discontinuous. The vapour is distributed in the liquid in the form of bubbles. The occurrence of bubbly flow is supported by the continuous course of the experimental ε/Q_g curves. From the results of Section 3.5 it follows that the bubbly flow reaches steady-state very quickly. It is likely that the experimental ε is equal to the voidage in the bulk solution just above the upper edge of the gas-evolving electrode.

From Fig. 3 it follows that a maximum gas voidage can be determined. Moreover, it was found that ε_{\max} is independent of the nature of the gas, the KOH-concentration and the volumetric flow rate of solu-

tion. The experimental ε_{\max} of 0.69 is higher than that for a stationary liquid [2], but smaller than that for chlorine bubbles in a 'gas bubble zone' in the upper part of the anodic compartment of a chlor-alkali cell [6].

It is likely that ε_{\max} is determined by the average bubble radius and the bubble radius distribution. Both quantities depend on two main factors, i.e. the departure radius of the bubbles from the electrode surface and the coalescence behaviour of the detached bubbles in the electrolyte. Bongenaar [7] found that the bubble radius distribution curves for oxygen and hydrogen bubbles, evolved on a nickel electrode in 30 wt % KOH, at the outlet of a gas-evolving cell are similar in the absence of bubble coalescence in the bulk of solution. It has also been found that the average bubble radius for oxygen and hydrogen bubbles is of the same order of magnitude and that oxygen bubbles coalesce more easily than hydrogen bubbles. Since ε_{\max} obtained by extrapolation is independent of the nature of the gas (Fig. 3), it may be concluded that, under the applied experimental conditions, the occurrence of bubble coalescence does not significantly affect the $\varepsilon^{-1}/Q_g^{-1}$ curve.

Figures 4 and 5 show that the $\log(\varepsilon/(\varepsilon_{\max} - \varepsilon))/\log Q_g$ curves are practically independent of the nature of the gas bubbles and KOH concentration and their slope is 1.00. Moreover, from Figs 4 and 5 it can be deduced that under the experimental conditions of Figs 4 and 5 $\varepsilon/(\varepsilon_{\max} - \varepsilon) = 0.82 Q_g^{1.00}$, where $\varepsilon_{\max} = 0.69$ and Q_g is expressed in $\text{cm}^3 \text{s}^{-1}$.

Since the temperature effect on ε at a constant Q_g is negligible (Section 3.5), the temperature increase during the experiments with increasing current $I_{g,p}$ does not affect the relation between $\varepsilon/(\varepsilon_{\max} - \varepsilon)$ and Q_g as deduced from Figs 4 and 5, where corrections for the temperature increase have been taken into account.

The effect of solution flow rate is shown in Figs 8 and 9. The experimental ε under the most extreme experimental conditions, namely, at $Q_1 = 0.853 \text{ cm}^3 \text{s}^{-1}$ and $Q_g = 3.54 \text{ cm}^3 \text{s}^{-1}$ is much smaller than that found by extrapolation of the ε/Q_1 curve. In this case the conductivity measured shows extremely large fluctuations. This can be explained by the occurrence of slug flow at this very high Q_g/Q_1 ratio.

From Figs 8 and 9 it follows that for bubbly flow ε decreases with increasing Q_1 . In this Section it has been found that $\varepsilon/(0.69 - \varepsilon) = a_1 Q_g$, where the parameter a_1 depends on the flow rate. From the results of Figs 8 and 9 the parameter a_1 was calculated. It was found that a_1 was independent of Q_g . The average values of a_1 obtained from the experiments at $I_{g,p}$ of about 7.5 and 23 A, are plotted against Q_1 in Fig. 10 on a double logarithmic scale for both KOH solutions containing hydrogen and oxygen bubbles. From Fig. 10 it follows that the slope a_2 of the $\log a_1$ against $\log Q_1$ curve is practically independent of the nature of the evolved gas and the KOH concentration, $a_1 = 1.40 Q_1^{-1.00}$, where Q_1 is given in $\text{cm}^3 \text{s}^{-1}$. Summarizing the results gives the relation

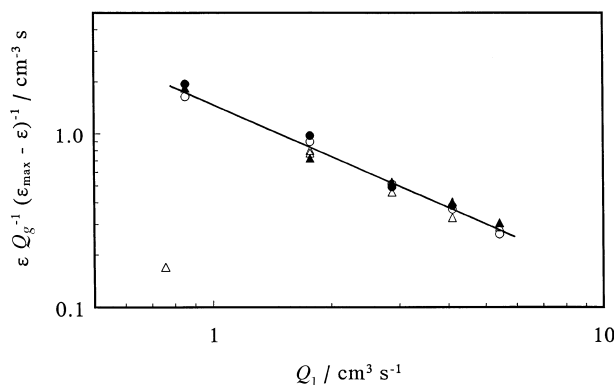


Fig. 10. Plot of parameter a_1 being $[(\varepsilon/\varepsilon_{\max} - \varepsilon)]/Q_g$ against Q_1 on a double logarithmic scale for a 10 (Δ , \blacktriangle) and a 26 wt % (\circ , \bullet) KOH solution containing hydrogen (Δ , \circ) and oxygen (\blacktriangle , \bullet) bubbles, where $\varepsilon_{\max} = 0.69$. The parameter a_1 was obtained from Figs 8 and 9.

$\varepsilon/(0.69 - \varepsilon) = 1.40 Q_g Q_1^{-1.00}$. Moreover, ε from this relation is equal to the voidage of bulk solution, ε_{∞} .

This relation has been obtained under bubbly flow conditions for hydrogen and oxygen evolving cell compartments with a dilute and a concentrated KOH solution as electrolytes. Since the behaviour of hydrogen and oxygen bubbles in alkaline solution are quite different, it is likely that the above relation for ε can also be applied to other gas-evolving systems, for instance hydrogen and oxygen evolution in acidic solutions and chlorine evolution in slightly acidic solutions.

Equation 9 from [1] describes the effect of voidage in the bulk solution on the voidage in the bubble layer at a gas-evolving electrode. Using this relation and the relation for ε_{∞} of this paper, the voidage distribution can be described and used to calculate the current distribution in the gas-evolving cell. The ohmic resistance distribution and thus the current distribution in the gas-evolving cell can be calculated, if the temperature profile in the cell is well-known. Particularly in industrial electrolyzers with a liquid inlet at the cell bottom and a liquid outlet at the cell top, and at low flow rates of solution the temperature increases from bottom to top in the cell will increase the solution conductivity. This counteracts the effect of increasing voidage, resulting in a levelling of the current distribution.

References

- [1] M. P. M. G. Weijs, L. J. J. Janssen and G. J. Visser, *J. Appl. Electrochem.* **27** (1997) 371.
- [2] M. Kuhn and G. Kreysa, *J. Appl. Electrochem.* **14** (1984) 653.
- [3] L. J. J. Janssen and G. J. Visser, *ibid.* **21** (1991) 386.
- [4] L. J. J. Janssen and E. Barendrecht, *Electrochim. Acta* **30** (1985) 683.
- [5] L. R. Czarnetzki and L. J. J. Janssen, *J. Appl. Electrochem.* **19** (1989) 630.
- [6] H. Shiroki, Y. Noaki, M. Katayose and A. Kashiwada, in 'Modern Chlor-Alkali Technology, Vol.6 (edited by R. W. Curry), The Royal Society of Chemistry, (1995), p. 222.
- [7] B. E. Bongeman-Schleuter, PhD thesis, Eindhoven University of Technology, NL (1984).